Inorg. Chem. **2006**, *45*, 2788–2794

Synthesis, Structures, and Luminescent Properties of Phenol–Pyridyl Boron Complexes

Hongyu Zhang, Cheng Huo, Kaiqi Ye, Peng Zhang, Wenjing Tian, and Yue Wang*

Key Laboratory for Supramolecular Structure and Materials of Ministry of Education, College of Chemistry, Jilin University, Changchun 130012, People's Republic of China

Received October 31, 2005

Syntheses of the four mixed phenol–pyridine derivatives 1,6-bis(2-hydroxyphenyl)pyridyl boron naphthalene (**1**), 1,6-bis(2-hydroxy-5-methylphenyl)pyridyl boron naphthalene (**2**), 1,6-bis(2-hydroxyphenyl)pyridyl boron 2-methoxylbenzene (**3**), and 1,6-bis(2-hydroxy-5-methylphenyl)pyridyl boron 2-methoxylbenzene (**4**) are reported. The structures of the boron compounds **1**, **3**, and **4** were determined by single-crystal X-ray diffraction. The molecular packing is characterized by intermolecular $\pi\cdots\pi$ and hydrogen-bonding interactions. DSC analysis demonstrates that **1** and **2** have good thermal stability with higher glass transition temperatures (T_g) and melting points (T_m) than **3** and **4**. Boron complexes **1**–**4** display bright blue luminescence in solution and the solid state. White and blue electroluminescent (EL) devices were fabricated successfully using these boron compounds.

Introduction

Polypyridines are widely used as polydentate chelating ligands that play a major role in the current intense interest in coordination chemistry. The coordination chemistry of polydentate chelating ligands that contain mixed pyridine−phenol donor sets has been a very popular target of study and is a possible extension to the chemistry of polypyridines. Ward and co-workers performed early studies of the complexes based on the mixed-donor polydentate ligands.[1−4] Recently, much effort has been invested in the design and synthesis of boron-containing compounds because of their potential applications in functional materials, including organic light-emitting devices (OLEDs), nonlinear optics, fluorescent and fluoride ion sensors, and biomolecular probes.[5−12] Wang and co-workers have systematically reported the syntheses, structures, and photoluminescent (PL) and electroluminescent (EL) properties of boron-containing compounds.[13] In view of the important potential applications of boron-containing compounds in OLEDs, we have explored the synthesis of novel four-coordinate boron complexes that contain the mixed phenol−pyridyl functional group.[14−16] These boron complexes are easy to handle in conventional vacuum deposition equipment. The following properties are

* To whom correspondence should be addressed. E-mail: yuewang@jlu.edu.cn.

(1) Jeffery, J. C.; Schatz, E.; Ward, M. D. *J. Chem. Soc., Dalton. Trans*. **1992**, 1921.
(2) Holligan, B. M.; Jeffery, J. C.; Norgett, M. K.; Scnatz, E.; Ward, M. D. *J. Chem. Soc., Dalton Trans.* **1993**, 2321
(3) Jeffery, J. C.; Thornton, P.; Ward, M. D. *Inorg. Chem.* **1994**, *33*, 3612.
(4) Holligan, B. M.; Jeffery, J. C.; Norgett, M. K.; Schatz, E.; Ward, M. D. *J. Chem. Soc., Dalton. Trans.* **1992**, 3345.
(5) (a) Noda, T.; Shirota, Y. *J. Am. Chem. Soc*. **1998**, *120*, 9714. (b) Noda, T.; Ogawa, H.; Shirota, Y. *Adv. Mater*. **1999**, *11*, 283. (c) Shirota, Y.; Kinoshita, M.; Noda, T.; Okumota, K.; Ohara, T. *J. Am. Chem. Soc*. **2000**, *122*, 11021. (d) Kinoshita, M.; Kita, H.; Shirota, Y. *Adv. Funct. Mater*. **2002**, *12*, 780. (e) Doi, H.; Kinoshita, M.; Okumota, K.; Shirota, Y. *Chem. Mater*. **2003**, *15*, 1080.
(6) (a) Wu, Q. G.; Wu, G.; Brancaleon, L.; Wang, S. *Organometallics* **1999**, *18*, 2553. (b) Liu, S.-F.; Wu, Q.; Schmider, H. L.; Aziz, H.; Hu, N.-X.; Popovic, Z.; Wang, S. *J. Am. Chem. Soc.* **2000**, *122*, 3671. (c) Liu, S.-F.; Seward, C.; Aziz, H.; Hu, N.-X.; Popovic, Z.; Wang, S. *Organometallics* **2000**, *19*, 5709. (d) Jia, W.-L.; Song, D.; Wang, S. *J. Org. Chem*. **2003**, *68*, 701. (e) Jia, W. L.; Moran, M. J.; Yuan, Y.-Y.; Lu, Z. H.; Wang, S. *J. Mater. Chem*. **2005**, *15*, 3326.
(7) (a) Yuan, Z.; Taylor, N. J.; Marder, T. B.; Williams, I. D.; Kurtz, S. K.; Cheng, L.-T. *J. Chem. Soc., Chem. Commun.* **1990**, 1489. (b) Yuan, Z.; Collings, J. C.; Taylor, N. J.; Marder, T. B.; Jardin, C.; Halet, J.-F. *J. Solid State Chem.* **2000**, *154*, 5. (c) Entwistle, C. D.; Marder, T. B.; Smith, P. S.; Howard, J. A. K.; Fox, M. A.; Mason, S. A. *J. Organomet. Chem*. **2003**, *680*, 165.
(8) (a) Branger, C.; Lequan, M.; Lequan, R. M.; Large, M.; Kajzar, F. *Chem. Phys. Lett*. **1997**, *272*, 265. (b) Branger, C.; Lequan, M.; Lequan, R. M.; Barzoukas, M.; Fort, A. *J. Mater. Chem*. **1996**, *6*, 555.
(9) (a) Allbrecht, K.; Kaiser, V.; Boese, R.; Adams, J.; Kaufmann, E. *J. Chem. Soc., Perkin Trans. 2* **2000**, 2153. (b) Yamaguchi, S.; Akiyama, S.; Tamao, K. *J. Am. Chem. Soc*. **2001**, *123*, 11372. (c) Kubo, Y.; Yamamoto, M.; Ikeda, M.; Takeuchi, M.; Shinkai, S.; Yamaguchi, S.; Tamao, K. *Angew. Chem., Int. Ed*. **2003**, *42*, 2036.
(10) (a) Yamaguchi, S.; Akiyama, S.; Tamao, K. *J. Am. Chem. Soc*. **2000**, *122*, 6335. (b) Yamaguchi, S.; Akiyama, S.; Tamao, K.; *J. Am. Chem. Soc*. **2001**, *123*, 11372. (c) Yamaguchi, S.; Akiyama, S.; Tamao, K. *J. Organomet. Chem.* **2002**, *652*, 3.
(11) Yang, W.; He, H.; Drueckhammer, D. G. *Angew. Chem., Int. Ed*. **2001**, *40*, 1714.

10.1021/ic051881j CCC: $33.50
Published on Web 01/13/2006

strongly required or indispensable for molecular EL materials: They must (a) form a uniform thin film, (b) have a carrier (hole or electron) transport ability, (c) have a high fluorescent yield, (d) be stable to heat (have a high glass transition temperature, T_g), and (e) have suitable HOMO/LUMO levels for carrier injections. To improve the performance of the boron compounds, we modified the boron molecules by attaching aromatic groups to the boron center. Herein, we report the details of our investigation on synthetic efforts; structures; and thermal, PL, and EL properties of a series of pyridine−phenol boron complexes.

Experimental Section

Materials. All starting materials were purchased from Aldrich Chemical Co. and used without further purification. Solvents were freshly distilled over appropriate drying reagents. All experiments were carried out under a dry nitrogen atmosphere using standard Schlenk techniques unless otherwise stated. The synthetic procedures of four-coordinate boron compounds **1**−**4** are shown in Scheme 1. *N*,*N*′-di(1-naphthyl)-*N*,*N*′-diphenyl-(1,1′-biphenyl)-4,4′-diamine) (NPB),[17] 4,4′-*N*,*N*′-dicarbazolebiphenyl (CBP),[17] 2,6-bis-(2-hydroxylphenyl)pyridine (H_2L1), and 2,6-bis(2-hydroxyl-5-methylphenyl)pyridine (H_2L2)[15] were synthesized according to the literature procedures. Aromatic-substituted boronic acids naphthylboronic acid (NBA) and 2-methoxylphenylboronic acid (MPBA) were prepared in high yield in a method analogous to the synthesis of 4-(dimethylamino)-naphthalene boronic acid (DMANBA) and phenylboronic acid.[18] Tri(8-hydroxyquinolino)aluminum (Alq_3) was purchased from Aldrich and purified by vacuum sublimation.

Instrumentation. ^{1}H NMR spectra were recorded on Bruker AVANCE 500-MHz spectrometer with tetramethylsilane as the internal standard. Mass spectra were recorded on a GC/MS mass spectrometer. UV−vis absorption spectra were obtained on a PE UV−vis lambdazo spectrometer. Emission spectra were recorded with a Shimadzu RF-5301 PC spectrometer. Elemental analyses were performed on a flash EA 1112 spectrometer. The EL spectra, luminance, and Commission Internationale del l'Eclairage (CIE) coordinates of the devices were recorded on a PR650 spectrometer. The melting points were determined on a Fisher-Johns melting point apparatus. Differential scanning calorimetric (DSC) measurements were performed on a NETZSCH DSC204 instrument.

1,6-Bis(2-hydroxyphenyl)pyridyl Boron Naphthalene (1). NBA (0.60 g, 3.5 mmol), H_2L1 (0.95 g, 3.6 mmol), and NEt_3 (1.5 mL) were dissolved in 30 mL of benzene, and the reaction mixture

Scheme 1. Synthetic Procedure for Boron Compounds **1**−**4**

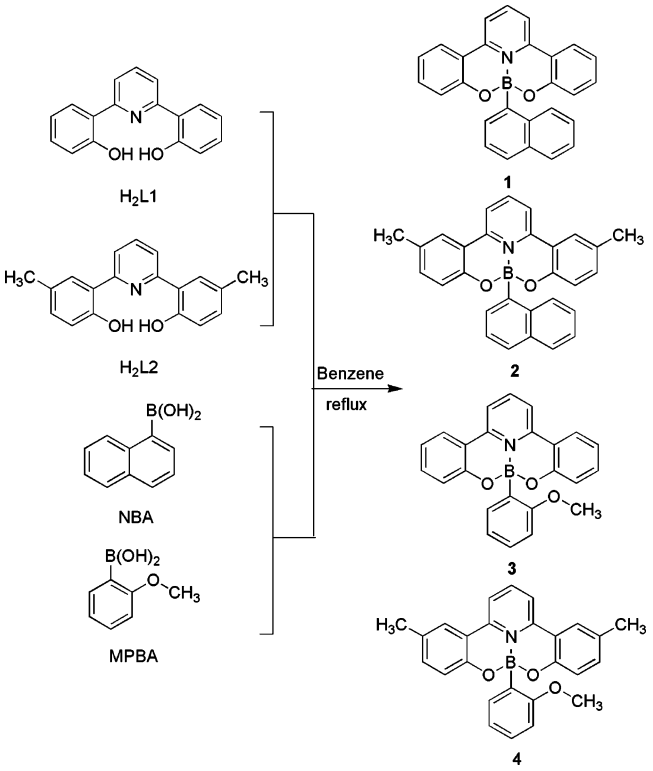

was heated to reflux for 10 h. A light yellow solid precipitated from the solution. The solid product was collected by filtration and purified by recrystallization and sublimation to give a light yellow solid (1.18 g, yield 80%). ^{1}H NMR ($CDCl_3$): δ (ppm) 9.12 (d, J = 8.0 Hz, 1H, naph), 8.12 (t, J = 8.0 Hz, 1H, py), 7.86 (d, J = 8.0 Hz, 2H, py), 7.64−7.70 (t, J = 7.0 Hz, 3H, naph, ph), 7.56 (t, J = 8.0 Hz, 1H, naph), 7.49 (d, J = 8.0 Hz, 1H, naph), 7.39 (t, J = 7.0 Hz, 1H, naph), 7.19 (t, J = 7.0 Hz, 2H), 6.94 (t, J = 8.0 Hz, 3H, naph, ph), 6.80 (t, J = 7.5 Hz, 2H), 6.32 (d, J = 5.0 Hz, 1H, naph). MS m/z: 399 $[M]^+$. Anal. Calcd (%) for $C_{27}H_{18}BNO_2$: C, 81.22; H, 4.54; N, 3.51. Found: C, 81.05; H, 4.75; N, 3.47. X-ray-quality crystals were grown by slow diffusion of diethyl ether vapor into a $CHCl_3$ solution of **1**.

1,6-Bis(2-hydroxy-5-methylphenyl)pyridyl Boron Naphthalene (2). In the same manner as described for **1**, the reaction of NBA (0.80 g, 4.6 mmol), H_2L2 (1.38 g, 4.7 mmol), and NEt_3 (1.7 mL) provided **2** as a light yellow solid (1.05 g, yield 53%). ^{1}H NMR ($CDCl_3$): δ (ppm) 9.09 (d, J = 8.5 Hz, 1H, naph), 8.09 (t, J = 8.0 Hz, 1H, py), 7.84 (d, J = 8.5 Hz, 2H, py), 7.65 (d, J = 8.0 Hz, 1H, naph), 7.54 (t, J = 7.5 Hz, 1H, naph), 7.48 (d, J = 8.5 Hz, 1H, naph), 7.42 (s, 2H, ph), 7.38 (t, J = 7.5 Hz, 1H, naph), 6.99 (d, J = 8.5 Hz, 2H, ph), 6.94 (t, J = 7.5 Hz, 1H, naph), 6.82 (d, J = 8.0 Hz, 2H, ph), 6.33 (d, J = 6.0 Hz, 1H, naph), 2.20 (s, 6 H). MS m/z: 427 $[M]^+$. Anal. Calcd (%) for $C_{29}H_{22}BNO_2$: C, 81.51; H, 5.19; N, 3.28. Found: C, 81.35; H, 5.12; N, 3.47.

1,6-Bis(2-hydroxyphenyl)pyridyl Boron 2-Methoxylbenzene (3). In the same manner as described for **1**, the reaction of MPBA (0.50 g, 3.3 mmol), H_2L1 (0.89 g, 3.4 mmol), and NEt_3 (1.5 mL) provided **3** as a light yellow solid (0.82 g, yield 66%). ^{1}H NMR ($CDCl_3$): δ (ppm) 8.04 (t, J = 7.5 Hz, 1H, py), 7.79 (d, J = 8.0 Hz, 2H, py), 7.68 (d, J = 8.0 Hz, 2H, ph), 7.34 (t, J = 8.5 Hz, 2H, ph), 7.22 (d, J = 7.0 Hz, 1H, ph), 7.09 (d, J = 7.5 Hz, 2H, ph), 7.00 (t, J = 8.0 Hz, 1H, ph), 6.87 (t, J = 8.0 Hz, 2H, ph), 6.69 (t, J = 7.5 Hz, 1H, ph), 6.55 (d, J = 8.0 Hz, 1H, ph), 3.28 (s, 3H, methoxyl). MS m/z: 379 $[M]^+$. Anal. Calcd (%) for $C_{24}H_{18}BNO_3$:

(12) (a) Yuan, Z.; Taylor, N. J.; Ramachandran, R.; Marder, T. B. *Appl. Organomet. Chem.* **1996**, *10*, 305. (b) Yamaguchi, S.; Shirasaka, T.; Tamao, K. *Org. Lett.* **2000**, *2*, 4129.
(13) (a) Wu, Q.; Esteghamatian, M.; Hu, N.-X.; Popovic, Z.; Enright, G.; Tao, Y.; Diorio, M.; Wang, S. *Chem. Mater.* **2000**, *12*, 79. (b) Liu, Q.; Mudadu, M. S.; Schmider, H.; Thummel, R.; Tao, Y.; Wang, S. *Organometallics* **2002**, *21*, 4743. (c) Jia, W. L.; Feng, X. D.; Bai, D. R.; Lu, Z. H.; Wang, S.; Vamvounis, G. *Chem. Mater.* **2005**, *17*, 164. (d) Liu, Q.-D.; Mudadu, M. S. Thummel, R.; Tao, Y.; Wang, S. *Adv. Funct. Mater.* **2005**, *15*, 143.
(14) (a) Li, Y. Q.; Liu, Y.; Bu, W. M.; Lu, D.; Wu, Y.; Wang, Y. *Chem. Mater.* **2000**, *12*. 2672. (b) Chen, J. S.; Ma, D. G.; Liu, Y.; Wang, Y. *J. Phys. D: Appl. Phys.* **2005**, *38*, 3366.
(15) Li, Y. Q.; Liu, Y.; Bu, W. M.; Guo, J. H.; Wang, Y. *Chem. Commun.* **2000**, 1551.
(16) Feng, J.; Li, F.; Gao, W. B.; Liu, S. Y.; Liu, Y.; Wang, Y. *Appl. Phs. Lett.* **2001**, *78*, 3497.
(17) 30. Koren, A. B.; Curtis, M. D.; Kampf, J. W. *Chem. Mater*. **1998**, *10*, 2235.
(18) (a) Gao, X.; Zhang, Y.; Wang, B. *Org. Lett*. **2003**, *24*, 4615. (b) Hebel, A.; Haag, R. *J. Org. Chem.* **2002**, *67*, 9452.

C, 76.01; H, 4.78; N, 3.69. Found: C, 76.27; H, 4.75; N, 3.57. X-ray-quality crystals were grown by slow diffusion of diethyl ether vapor into a $CHCl_3$ solution of **3**.

1,6-Bis(2-hydroxy-5-methylphenyl)pyridyl Boron 2-Methoxylbenzene (4). In the same manner as described for **1**, the reaction of MPBA (0.60 g, 3.9 mmol), H_2L2 (1.16 g, 4.0 mmol), and NEt_3 (1.5 mL) provided **4** as a light yellow solid (0.97 g, yield 61%). ^{1}H NMR ($CDCl_3$): δ (ppm) 7.97 (t, J = 8.0 Hz, 1H, py), 7.74 (d, J = 8.0 Hz, 2H, py), 7.44 (s, 2H, ph), 7.19 (d, J = 7.5 Hz, 1H, ph), 7.13 (d, J = 8.5 Hz, 2H, ph), 6.99 (t, J = 8.0 Hz, 1H, ph), 6.97 (d, J = 8.5 Hz, 2H, ph), 6.68 (t, J = 7.0 Hz, 1H, ph), 6.55 (d, J = 8.0 Hz, 1H, ph), 3.30 (s, 3H, methoxyl), 2.28 (s, 6 H, methyl). MS: m/z: 407 $[M]^+$. Anal. Calcd (%) for $C_{26}H_{22}BNO_3$: C, 76.68; H, 5.44; N, 3.44. Found: C, 76.59; H, 5.58; N, 3.47. X-ray-quality crystals were grown by slow diffusion of diethyl ether vapor into a pyridine solution of **4**.

Electrochemical Measurements. Redox potentials were measured by cyclic voltammetry using a three-electrode configuration on a BAS 100W instrument with scan rates of 100 mV/s. The working electrode was a platinum wire, and a platinum wire and a saturated calomel electrode (SCE) served as the counter and reference electrodes, respectively. A 0.1 M solution of tetrabutylammonium perchlorate (TBAP) in DMF was used as the supporting electrolyte and was flushed with N_2 prior to the measurements to avoid oxygen contamination.

PL Quantum Yield Measurements. Room-temperature luminescence quantum yields were measured at a single excitation wavelength (360 nm) referenced to quinine sulfate in sulfuric acid aqueous solution (Φ = 0.546). The quantum yields were calculated using previously known procedures.[19] The excitation wavelength was 346 nm for all boron compounds **1**−**4**.

Fabrication of EL Devices. Indium tin oxide- (ITO-) coated glass was used as the substrate. It was cleaned by sonication successively in a detergent solution, acetone, and deionized water, followed by air-plasma treatment. The devices were prepared in a vacuum at a pressure of 5×10^{-6} Torr, and the organic materials were deposited onto indium tin oxide at a deposition rate of 1−2 Å/s. Aluminum electrodes were thermally evaporated onto the organic surface, resulting in active areas of ~5 mm^2. The thicknesses of the organic materials and cathode layers were controlled using a quartz crystal thickness monitor. The electrical characteristics of the diode were measured with a Keithley 2400 source meter.

X-ray Diffraction. Diffraction data were collected on a Rigaku RAXIS-PRID diffractometer using the ω-scan technique with graphite-monochromated Mo·Kα (λ = 0.71073 Å) radiation. The structures were solved by direct methods and refined by the full-matrix least-squares technique using the SHELXTL programs. Anisotropic displacement parameters were applied to all nonhydrogen atoms, hydrogen atoms were assigned isotropic displacement coefficients. Crystal data and details of data collection and refinement for compounds **1**, **3**, and **4** are summarized in Table 1.

Results and Discussion

Single-Crystal Structures. The solid-state structures of molecular functional materials have a pronounced impact on their physical properties, especially luminescent and charge-transport properties.[20,21] To understand the relationship between the properties and structures of functional materials, the crystal structures of the synthesized complexes were investigated. The crystallographic data for **1**, **3**, and **4** are given in Table 1. Selected bond lengths and angles are listed in Table 2. Even though all of the boron compounds have similar structures, they crystallize in different space groups. **1** belongs to the monoclinic space group $P2_1/c$, **3** belongs to the triclinic space group $P\bar{1}$, **4** belongs to the monoclinic

Table 1. Crystal Data for Compounds **1**, **3**, and **4**

	1	**3**	**4**
formula	$C_{54}H_{36}B_2N_2O_4$	$C_{25}H_{19}BCl_3NO_3$	$C_{31}H_{27}BN_2O_3$
fw	798.47	498.57	486.36
crystal system	monoclinic	triclinic	monoclinic
space group	$P2_1/c$	$P\bar{1}$	$P2/n$
a (Å)	15.033(3)	9.309(2)	7.626(2)
b (Å)	27.353(6)	11.609(2)	25.956(5)
c (Å)	10.260(2)	12.000(2)	13.249(3)
α (deg)	90	65.96(3)	90
β (deg)	108.50(3)	74.95(3)	104.34(3)
γ (deg)	90	75.20(3)	90
V (Å)	4000.9(14)	1127.2(4)	2540.8(9)
Z	4	2	4
D_c (g cm^{-3})	1.326	1.469	1.271
θ_{max} (deg)	27.48	27.44	27.48
no. of reflns meads	8247	5060	5946
no. of reflns used	8084	5060	5801
no. of parameters	559	298	334
R(int)	0.0546	0.02	0.04
final R indices [$I > 2d(I)$]			
R1	0.049	0.043	0.044
wR	0.104	0.122	0.091
R indices (all data)			
R1	0.187	0.095	0.158
wR2	0.16	0.146	0.142
GOF on F^2	0.715	0.807	0.767

Table 2. Selected Bond Lengths (Å) and Angles (deg) for Compounds **1**, **3**, and **4**

	1	**3**	**4**
B(1)−O(1)	1.447(4)	1.442(3)	1.478(3)
B(1)−O(2)	1.459(4)	1.477(3)	1.460(3)
B(1)−N(1)	1.594(5)	1.605(3)	1.613(3)
B(1)−C(18)	1.614(5)	1.617(4)	1.624(4)
O(2)−C(17)	1.339(4)	1.348(3)	1.354(3)
O(1)−C(1)	1.349(4)	1.343(3)	1.357(3)
N(1)−C(11)	1.352(4)	1.357(3)	1.371(3)
N(1)−C(7)	1.376(4)	1.358(3)	1.374(3)
O(1)−B(1)−O(2)	105.0(3)	105.4(2)	105.3(2)
O(1)−B(1)−N(1)	107.9(3)	109.1(2)	106.2(2)
O(2)−B(1)−N(1)	106.6(3)	104.9(2)	108.7(2)
O(1)−B(1)−C(18)	113.3(3)	114.0(2)	111.0(2)
O(2)−B(1)−C(18)	114.3(3)	111.3(2)	113.2(2)
N(1)−B(1)−C(18)	109.3(3)	111.6(2)	111.9(2)
C(17)−O(2)−B(1)	116.2(3)	114.4(2)	122.9(2)
C(1)−O(1)−B(1)	118.8(3)	122.6(2)	115.9(2)
C(11)−N(1)−C(7)	122.8(3)	121.4(2)	120.7(2)
C(11)−N(1)−B(1)	118.3(3)	116.6(2)	122.0(2)
C(7)−N(1)−B(1)	118.8(3)	122.2(2)	117.3(2)
O(1)−C(1)−C(2)	118.8(4)	117.9(2)	119.4(3)
O(1)−C(1)−C(6)	120.3(4)	122.1(2)	121.0(2)

(19) Ye, K.; Wang, J.; Sun, H.; Liu, Y.; Mu, Z.; Li, F.; Jiang, S.; Zhang, J.; Zhang, H.; Wang, Y.; Che, C. M. *J. Phys. Chem. B* **2004**, *109*, 8008.

(20) (a) Liu, B.; Yu, W.; Lai, Y.; Huang, W. *Chem. Commun*. **2000**, 551. (b) Ma, C. Q.; Zhang, L. Q.; Zhou, J. H.; Wang, X. S.; Zhang, B. W.; Cao, Y.; Bugnon, P.; Schaer, M.; Nuesch, F.; Zhang, D. Q.; Qiu, Y. *J. Mater. Chem.* **2002**, *12*, 3481.

(21) (a) Brinkmann, M.; Gadret, G.; Muccini, M.; Taliani, C.; Masciocchi, N.; Sironi, A. *J. Am. Chem. Soc.* **2000**, *122*, 5147. (b) Antolini, L.; Tedesco, E.; Barbarella, G.; Favaretto, L.; Sotgiu, G.; Zambianchi, M.; Casarini, D.; Gigli, G.; Cingolani, R. *J. Am. Chem. Soc*. **2000**, *122*, 9006.

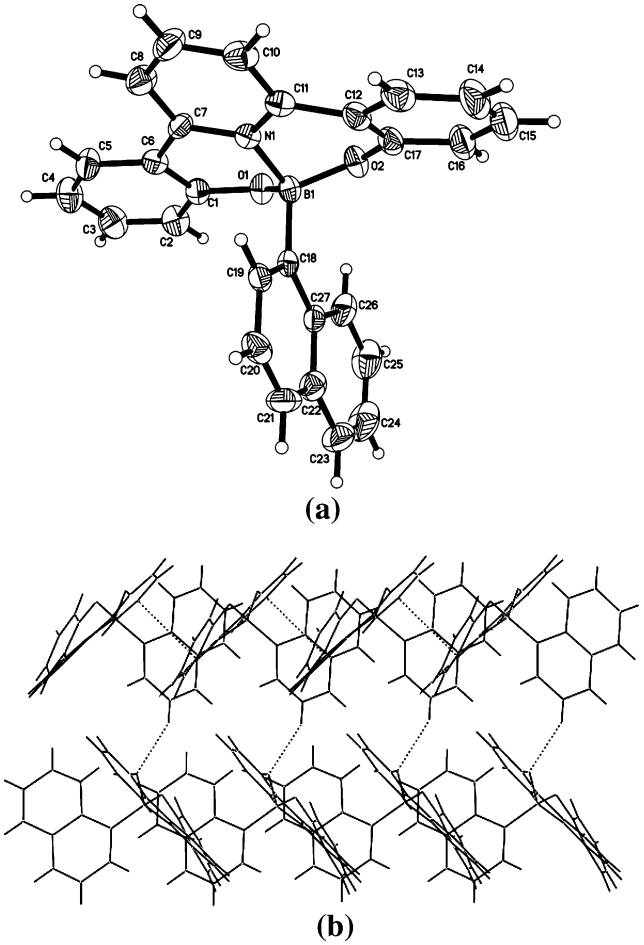

Figure 1. (a) Molecular structure with labeling scheme and (b) stereoview of the crystal packing of **1**.

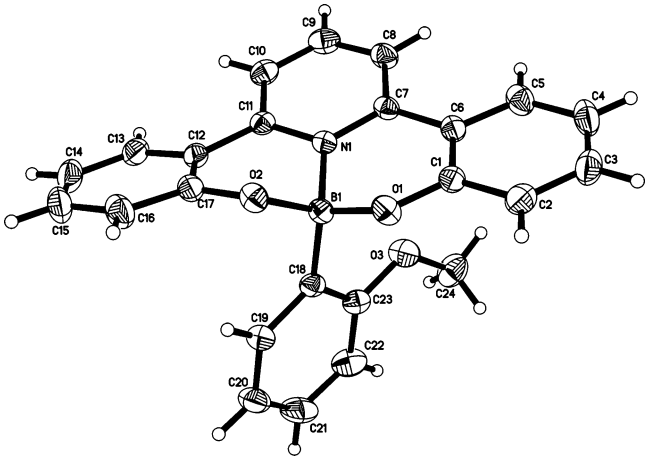

Figure 2. Molecular structure with labeling scheme of **3**.

space group *P*2/*n*, The molecular structures of **1**, **3**, and **4** are very similar to each other. The ORTEP drawings of **1**, **3**, and **4** are given in Figures 1a, 2, and 3a, respectively. For **1**, in the asymmetric unit, there are two independent molecules that display the same structure; the B−N, B−O, and B−C distances and angles for the two molecules are very similar to each other. For **3** and **4**, the two structures contain one crystallographically independent molecule. The boron centers in all of the compounds are four-coordinate and adopt a typical tetrahedral geometry. Each boron center

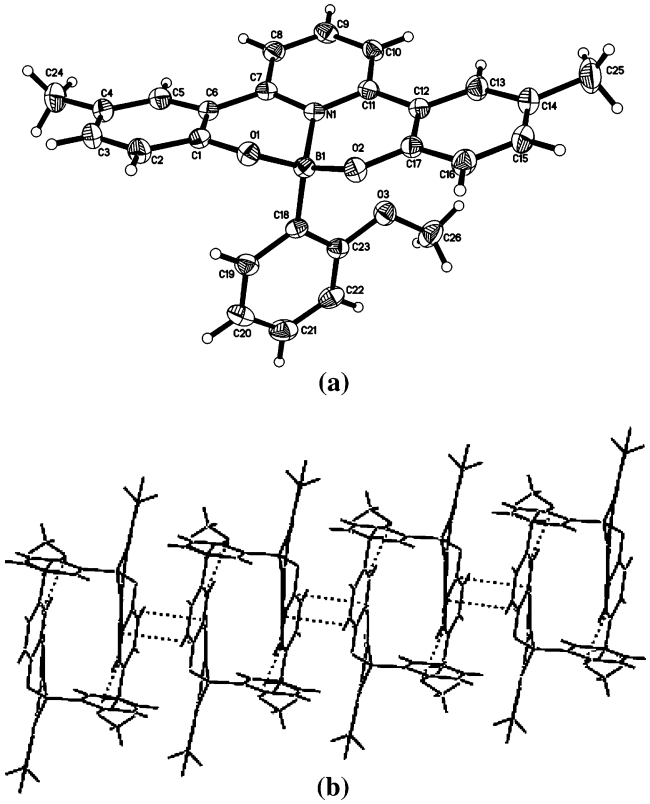

Figure 3. (a) Molecular structure with labeling scheme and (b) stereoview of the crystal packing of **4**.

is chelated in a tridentate fashion by ligand (L1 for **1** and **3** and L2 for **4**, respectively) via O1, O2, and N1; the remaining site is occupied by the aromatic group. In all of the compounds, each ligand (L1 or L2) is slightly distorted from planarity with inter-ring torsion angles between the pyridyl ring and the phenolate rings in the range of 4.46−20.07° (14.45° and 19.53° for **1**, 7.59° and 20.07° for **3**, and 4.46° and 16.53° for **4**). The molecular packing of the boron compounds in the solid state exhibits interesting features.

The crystal packing diagram given in Figure 1b shows that **1** has a chain arrangement in the solid state. Within each chain, there is a $\pi-\pi$ stacking interaction with a pyridyl/phenolate ring contact distance of 3.40 Å that is longer than that in solid (dppy)BF (3.28 Å);[15] the increase in the $\pi-\pi$ interaction distance might be due to the large steric hindrance of the naphthyl group. Two molecular chains are linked by a C−H···O hydrogen bond at a distance of 2.465 Å, resulting in a chain dimmer. For molecular semiconducting materials, strong intermolecular aromatic stacking interactions can enhance the charge-transfer ability.[22] Our earlier reports also demonstrated that the higher electron mobility of tris(8-hydroxyquinolinato)gallium[23] and $Be(pp)_2$[14] is due to intermolecular $\pi-\pi$ stacking interactions. It is possible that the strong intermolecular $\pi-\pi$ stacking interaction accompanied by a hydrogen bond in solid **1** is beneficial in terms of charge

(22) (a) Munakata, M.; Wu, L. P.; Sowa, T. K.; Maekawa, M.; Suenaga, Y.; Ning, G. L.; Kojima, T. *J. Am. Chem. Soc.* **1998**, *120*, 8610. (b) Cornil, J.; Calbert, J-P.; Beljonne, D.; Silbey, R.; Bredas, J. L. *Adv. Mater.* **2000**, *12*, 978.
(23) Wang, Y.; Zhang, W. X.; Li, Y. Q.; Ye, L.; Yang, G. D. *Chem. Mater.* **1999**, *11*, 530.

Table 3. Thermal and Redox Properties for Compounds **1**−**4**

compd	$E_{red}/2$ (V)	E_{HOMO} (eV)	E_{LUMO} (eV)	band gap (eV)	T_g (°C)	T_m (°C)
1	−2.01	−5.62	−2.84	2.78	142	309
2	−2.13	−5.42	−2.72	2.70	139	312
3	−2.08	−5.54	−2.77	2.77		227
4	−2.07	−5.49	−2.78	2.71	104	208

mobility. In **3** and **4**, the molecular packing modes are very similar, with two molecules arrayed in a face-to-face fashion by $\pi\cdots\pi$ interactions at distances of 3.342 Å for **3** and 3.299 Å for **4**, resulting in the formation of molecular "dimmers". In **3**, the dimmers are isolated from each other, and no other short intermolecular contacts exist between the dimmers. However, in **4**, the dimmers are linked via hydrogen-bonded contact C4−H4···O3 at a distance of 2.713 Å and an angle of 156.54° (Figure 3b).

Thermal Behaviors. The glass transition temperatures (T_g) and melting point temperatures (T_m) of compounds **1**−**4** were determined by differential scanning calorimetry (DSC). A heating rate of 5 °C/min was used after initial melting of the compounds and subsequent rapid cooling to room temperature under ambient conditions. These compounds constitute a new class of amorphous molecular materials with T_g values of 142, 139, and 104 °C for **1**, **2**, and **4**, respectively. DSC shows no evidence of a glass transition for **3**. The T_g values significantly increase in the order phenyl < naphthyl; the results are in agreement with the concept that the introduction of a rigid moiety into nonplanar molecules increases the T_g value.[24] T_m values of 309, 312, 227, and 208 °C were observed for compounds **1**−**4**, respectively, and increase in the same order (phenyl < naphthyl) as T_g. The high T_m and T_g values are promising in view of the thermal stability of thin films in EL devices. The T_g and T_m values of all of the compounds are listed in Table 3.

Among these compounds, **1** and **4** were found to exhibit crystal polymorphism in addition to the formation of amorphous glasses. Figure 4 shows the DSC curves of **1**. When the crystalline sample (crystal **1a**) obtained by vacuum sublimation was heated from room temperature, it melted at 321 °C to give an isotropic liquid. When the isotropic liquid was cooled by standing in air, it changed into an amorphous glassy state via a supercooled liquid. When the amorphous glassy sample was again heated, an endothermic phenomenon was observed, and a glass transition took place at 142 °C. Then, a broad exothermic peak was observed around 236 °C, probably due to a solid−solid phase transition to form a different crystal form (crystal **1b**).[5d] Upon further heating, crystal **1b** melted at 309 °C to give an isotropic liquid. No crystallization was observed on further heating, and the same DSC trace was observed repeatedly. Figure 5 shows the DSC curves of **4**. When a crystalline sample (crystal **4a**) obtained by vacuum sublimation was heated, it melted at 208 °C and then instantly crystallized to form another crystal (crystal **4b**), which melted at 241 °C to give an isotropic liquid. When the isotropic liquid was cooled by standing in air, it changed into an amorphous glassy state via a supercooled liquid. When the amorphous glassy sample was again heated, an endothermic phenomenon was observed, and a glass transition took place at 104 °C. Then, a broad exothermic peak due to crystallization (crystal **4a**) was observed around 183 °C, followed by an endothermic peak due to the melting at 208 °C. No crystallization was observed on further heating, and the same DSC trace was observed repeatedly.

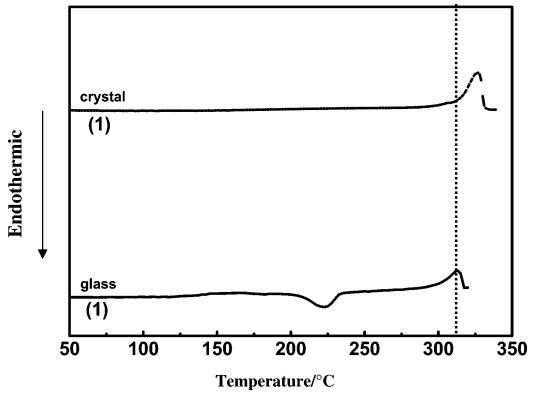

Figure 4. DSC curves of compound **1** at a heating rate of 5 °C/min.

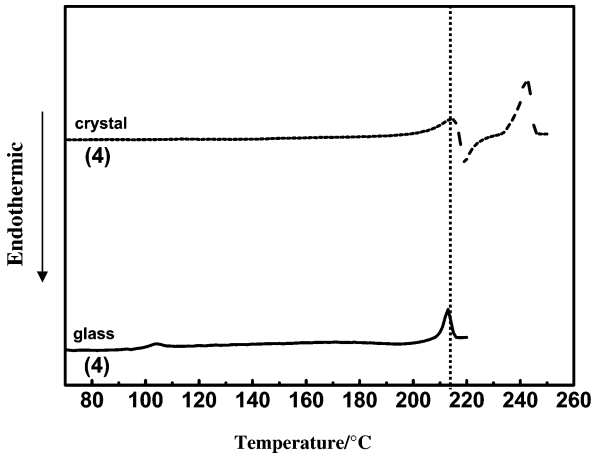

Figure 5. DSC curves of compound **4** at a heating rate of 5 °C/min.

Redox Properties and Energy Levels. The electrochemical properties of compounds **1**−**4** were investigated by cyclic voltammetry. All of these compounds display a reversible reduction peak in DMF at about −2.0 V, which is believed to originate from the reduction of the phenol−pyridyl boron moiety. No oxidation potentials could be obtained for this class of compounds in DMF. The half-wave reduction potentials ($E_{1/2}^{red}$) are almost all the same, being −2.01, −2.13, −2.08, and −2.07 V vs Ag/Ag^+ (0.01 M) for **1**−**4**, respectively. The results indicate that the electron-accepting properties of the compounds are almost the same as those of Alq_3 ($E_{1/2}^{red} = -2.01$ V vs Ag/Ag^+), suggesting that **1**−**4** might have electron-transport properties. Primary mobility measurements demonstrated that **1**−**4**, indeed, exhibit electron-transporting properties. The detailed experimental results will be published elsewhere. When the scan was repeated in the region between −2.5 and 1.0 V vs Ag/Ag^+ (0.01 M), the same trace was obtained. Using the reduction potentials of **1**−**4** and the absorption edges of the UV−vis spectra, we

(24) (a) Higuchi, A.; Inada, H.; Kobata, T.; Shirota, Y. *Adv. Mater*. **1991**, *3*, 549. (b) Okumoto, K.; Ohara, T.; Shirota, Y. *Synth. Met.* **2001**, *121*, 1655.

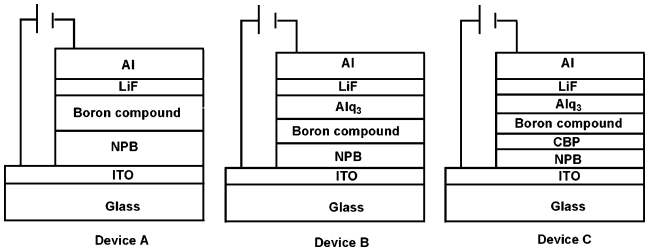

Figure 6. EL cell structures of devices A−C.

obtained the HOMO and LUMO energy levels, and the resulting data are also summarized in Table 3.

Photoluminescent Properties. The optical properties of boron compounds **1**−**4** were measured both in chloroform solution and in the solid state. The absorbance and emission spectra of compounds **1**−**4** in chloroform solution were measured at room temperature. All of these compounds show essentially similar absorption bands around 280−289, 338−352, and 382−393 nm. Upon irradiation by UV light (λ_{ext} = 365 nm), compounds **1**−**4** exhibit bright blue emissions in chloroform. The emission maxima of compounds **1**−**4** in chloroform are at 461, 478, 459, and 479 nm, respectively. These emissions are attributed to the intraligand $\pi \rightarrow \pi^*$ electron transition of L1 or L2. The emissions of compounds **2** and **4** with two electron-donating substituents (methyl groups) are red-shifted by 17 and 20 nm compared to those of **1** and **3**, respectively, reflecting the important role played by the methyl group in the phenol−pyridyl ligand. Emission quantum yields were measured for compounds **1**−**4**. Among these compounds, **1** has a quantum yield 0.30, significantly higher than those of **2** (0.21), **3** (0.16), and **4** (0.14). The low quantum yields of **3** and **4** are most likely due to the thermal motion of the conformationally mobile methoxy group, which results in energy loss via nonradiative decay.[13b,13d] In the solid state, the emissions of **1**−**4** are found at 454, 466, 449, and 462 nm, respectively. The emission spectra of **1**−**4** in the solid state exhibit slight blue shifts compared to those of **1**−**4** in solution. This phenomenon is probably due to luminescence rigidochromism.[25]

Electroluminescent Properties. Three types of devices with structures of [ITO/NPB (50 nm)/**1**−**4** (50 nm)/LiF (1 nm)/Al (200 nm)] (device A), [ITO/NPB (50 nm)/**1**−**4** (40 nm)/Alq_3 (10 nm)/LiF (1 nm)/Al (200 nm)] (device B), and [ITO/NPB (40 nm)/CBP (10 nm)/**1**−**4** (40 nm)/Alq_3 (10 nm)/LiF (1 nm)/Al (200 nm)] (device C) were fabricated (Figure 6). Figure 7 shows the molecular structures of the materials used in this study. The EL performance data for the devices are summarized in Table 4 for comparison.

The EL spectra of device A-1 are broad, ranging from 400 to 680 nm, which contains a blue emission peak and a orange one and completely covers the whole wavelength region of the visible spectrum; that is, white-light emission was obtained. It was demonstrated that high-performance white-light EL devices can be obtained by the rational combination of a blue emission and an orange emission.[26−28]

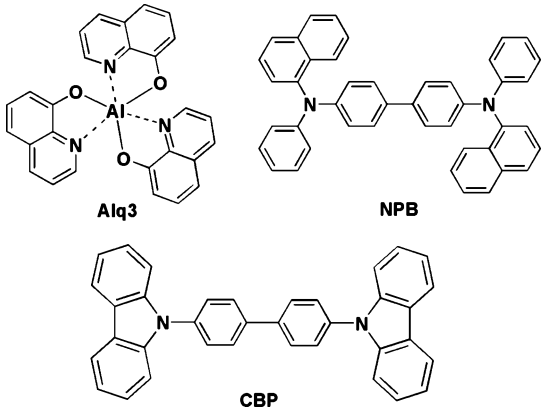

Figure 7. Molecular structures of Alq_3, NPB, and CBP.

Table 4. Performance of OLEDs of Compounds **1**−**4**

device	compd	T^a (V)	$L_{max}{}^b$ (Cd m^2)	$EI_{max}{}^c$ (Cd/A)	$EP_{max}{}^d$ (lm/W)	CIE^e (x, y)
A-1	**1**	3.0	1016	1.68	0.68	0.30, 0.37
A-2	**2**	3.2	792	1.47	0.59	0.28, 0.39
A-3	**3**	3.8	813	1.35	0.53	0.26, 0.36
A-4	**4**	4.7	648	1.27	0.52	0.22, 0.33
B-1	**1**	4.1	1852	2.39	1.17	0.26, 0.38
B-2	**2**	4.7	1323	1.71	0.79	0.27, 0.44
B-3	**3**	3.5	1537	2.01	0.95	0.27, 0.37
B-4	**4**	4.5	1271	1.62	0.7	0.20, 0.33
C-1	**1**	4.8	1171	1.55	0.87	0.17, 0.19
C-2	**2**	5.7	527	0.82	0.43	0.21, 0.27
C-3	**3**	5.5	494	1.01	0.57	0.18, 0.19
C-4	**4**	6.5	445	0.71	0.31	0.19, 0.29

[a] Turn-on voltage, defined as the voltage needed for a brightness of 1 Cd/m^2. [b] Maximum luminance. [c] Maximum current efficiency. [d] Maximum luminance efficiency. [e] CIE coordinates at a driving voltage of 8.0 V.

Table 4 shows the color coordinates of devices A and B, for example, and the values (0.28, 0.39) and (0.26, 0.38) deviate from the ideal CIE chromaticity coordinates for pure white light, (0.33, 0.33), this variation is attributed to the lack of sufficient red emission from these devices. In other words, these devices exhibit blue-white light emissions. The EL spectral component around 450 nm can be attributed to **1** or NPB. The EL band beyond the blue region is due to exciplex emissions. Electroluminescent devices using four-coordinate boron compounds as emitters can produce exciplex emissions and were demonstrated previously by us and other group.[13a,16] The EL spectral profile and the CIE coordinates (0.30, 0.38) remained almost unchanged when the driving voltage was varied. The EL spectra of device B-**1** change dramatically as a function of the applied bias. At high driving voltage (≥9 V), the device EL spectra resembled that of device A-**1**. At low driving voltage (4−8 V), the green emission intensity was stronger than the blue emission. This observation suggests that the electron−hole recombination zone in this device is field-dependent. Clearly, emission from device B-**1** is more pronounced with increasing driving voltage, indicating that CIE coordinates depend on driving voltage. For example, the CIE coordinates of device B-**1** with an Alq_3 thickness of 10 nm are (0.27, 0.40) and (0.25, 0.35) at 6 and 10 V, respectively.

(25) Kalyanasundaram, K. *Photochemistry of Polypyridine and Porphyrin Complexes*; Academic Press: London, 1992; pp 322−323.
(26) Li, G.; Shinar, J. *Appl. Phys. Lett.* **2003**, *83*, 5359.
(27) Shao, Y.; Yang, Y. *Appl. Phys. Lett.* **2005**, *86*, 1.
(28) Li, J. Y.; Liu, D.; Ma, C.; Lengyel, O.; Lee, C.-S.; Tung, C.-H.; Lee, S. *Adv. Mater.* **2004**, *16*, 1538.

To investigate the exciplex emission properties of the NPB/**1** system, solid thin films deposited on quartz substrates were employed to record the emissions spectra. The PL spectra of thin films of NPB and **1** show blue emissions with peaks at 443 and 465 nm. In contrast, the PL spectrum of a blend thin film of NPB/**1** (ca. 1:1 w/w) composite centered at 520 nm and red-shifted by 55 and 77 nm relative to those of neat films of **1** and NPB, respectively. The PL spectra of solid thin films confirm that the interaction between NPB and **1** molecules can result in exciplex emission.

Considering the possibility of exciplex emission between a layer of **1** and a layer of NPB, a second hole-transporting layer of CBP (4,4′-*N*,*N*′-dicarbazolebiphenyl) was inserted between NPB and **1**. In this case, the exciplex emission disappeared. Therefore, whereas exciplex emission occurs at the interface NPB and **1**, no exciplex emission takes place at the interface of CBP and **1**. This can be attributed to the proper HOMO energy level of CBP that is favorable for hole injection into the **1** layer to give an EL response that is dominated by emission of **1** at about 460 nm. The CBP layer provides an intermediate level for holes to transport through to the **1** layer. Two layers of hole-transporting materials NPB and CBP were used, as it was demonstrated previously that CBP serves to provide an intermediate HOMO level by which the holes can pass to the TPBI layer.[29]

The performance of the OLEDs of these materials is summarized in Table 4. The emissions from the white-emitting devices started at turn-on voltages of 3.0−4.7 V for devices of the A and B series. In the A series, the white-emitting device A-**1** exhibits a maximum luminance of 1016 Cd/m^2 at a driving voltage of 14 V (202 mA/cm^2), a current efficiency of 1.68 Cd/A at a luminance of 192 Cd/m^2, and a turn-on voltage as low as 3.0 V. With regard to the white-emitting devices in the B series, B-**1** exhibits better performance, with a maximum luminance of 1852 Cd/m^2 at a driving voltage of 14 V (415 mA/cm^2), a maximum luminous efficiency of 1.17 lm/W, and a maximum current efficiency of 2.39 Cd/A at a luminance of 152 Cd/m^2. It is obvious that the white-emitting devices in the B series are more efficient and have higher luminances than the white-emitting devices in the A series. We attribute the high luminance and EL efficiency in the three-layer device to enhanced electron transport and efficient radiative carrier recombination. In the C series, the blue-emitting device C-**1** exhibits a maximum luminance of 1171 Cd/m^2 at 11 V, a maximum current efficiency of 1.55 Cd/A, and CIE coordinates of (0.17, 0.19). The present study shows that the synthesized new amorphous boron compounds **1**−**4** can function as emitters as well as electron-transport materials for white- and blue-emitting materials in organic EL devices. **1** exhibits better EL performance in all three series of devices than **2**−**4**.

(29) Tao, Y. T.; Balasubramaniam, E.; Danel, A.; Tomasik, P. *Appl. Phys. Lett.* **2000**, *77*, 933.

Conclusions

The novel four-coordinate boron-containing amorphous molecular materials **1**−**4** have been synthesized. Single-crystal X-ray diffraction demonstrates that the molecular packing is sensitive to the aromatic groups attached to the boron center, although the molecular structures are very similar to each other among compounds **1**, **3**, and **4**. They readily form stable amorphous glasses with high T_g values and form uniform amorphous thin films by vacuum deposition. Compounds **1**−**4** show strong blue photoluminescence in solution and the solid state, and the luminescence of the boron compounds is caused by $\pi \rightarrow \pi^*$ electronic transitions centered on the phenol−pyridine ligands (L1 and L2). The naphthyl-substituted compound **1** appears to be the most promising as an emitter for EL displays.

Acknowledgment. This work was supported by the National Natural Science Foundation of China (50225313 and 50520130316), the Major State Basic Research Development Program (2002CB613401), and the Program for Changjiang Scholars and Innovative Research Team in University (IRT0422).

Supporting Information Available: Crystallographic data in CIF and PDF formats, Tables S1−S15, Figures S1−S12. This material is available free of charge via the Internet at http://pubs.acs.org.

IC051881J